

Molecular Docking and Dynamics of *Xylocarpus granatum* as A Potential Parkinson's Drug Targeting Multiple Enzymes

Riyan Alifbi Putera Irsal ^{1,2}  

Gusnia Meilin Gholam ^{1,3}   

Dzikri Anfasa Firdaus ^{1,2} 

Novian Liwanda ¹  

Fernanda Chairunisa ^{4*}  

¹ Department of Biochemistry, [Institut Pertanian Bogor](#), Bogor, West Java, Indonesia

² [Biomatics](#), Bogor, West Java, Indonesia

³ Bioinformatics Research Center, [Indonesian Institute of Bioinformatics](#), Malang, East Java, Indonesia

⁴ Department of Biology, [Universitas Nasional](#), South Jakarta, Special Capital Region of Jakarta, Indonesia

*email:

fernandachairunisa@civitas.unas.ac.id;

phone: +6281383388113

Keywords:

Adenosine A2A receptor

Catechol-O-methyltransferase

Monoamine oxidase-B

Neurology

Abstract

Parkinson's disease is a global health challenge affecting over 10 million individuals worldwide, leading to increased disability-adjusted life years (DALYs) and a rise in mortality rates. This study explores the potential anti-Parkinson's properties of *Xylocarpus granatum*, focusing on its interaction with key enzymes associated with the disease: catechol-O-methyltransferase (COMT), adenosine A2A receptor (A2AR), and monoamine oxidase-B (MAO-B). Using molecular docking and molecular dynamics approaches with YASARA Structure, the ethanol extract of *X. granatum* was investigated for its mechanism of action. Among 30 compounds, five demonstrated promising binding affinities. Structural flexibility analysis revealed minimal fluctuations in active-site residues, highlighting the stability of key complexes involving kaempferol, epicatechin, epigallocatechin, and native ligands. Molecular Mechanics Poisson-Boltzmann Surface Area (MM-PBSA) simulations provided insights into the binding energy of these complexes. Notably, kaempferol exhibited higher binding energy than the natural ligand, suggesting superior binding affinity. Analysis of the average radius of gyration (Rg) showcased control drug-MAO-B exhibited higher Rg values, indicating a more flexible protein conformation. Confirming mode stability with root mean square deviation (RMSD) analysis shows overall stability, except in the A2AR-bound complex. The study's collective findings underscore the structural stabilization of ligand-protein complexes, contributing valuable insights into the potential anti-Parkinson's properties of *X. granatum*. These discoveries hold promise for developing more effective therapies for Parkinson's disease and significantly contribute to the neurology field.

Received: March 8th, 2024

1st Revised: May 15th, 2024

Accepted: May 20th, 2024

Published: May 30th, 2024



© 2024 Riyan Alifbi Putera Irsal, Gusnia Meilin Gholam, Dzikri Anfasa Firdaus, Novian Liwanda, Fernanda Chairunisa. Published by [Institute for Research and Community Services Universitas Muhammadiyah Palangkaraya](#). This is an Open Access article under the CC-BY-SA License (<http://creativecommons.org/licenses/by-sa/4.0/>). DOI: <https://doi.org/10.33084/bjop.v7i2.6810>

INTRODUCTION

Parkinson's disease (PD) is a progressive neurodegenerative disorder affecting millions worldwide. Over 10 million people currently live with PD, with a significant rise in disease burden observed since 2000¹. This translates to a substantial increase in disability-adjusted life years (DALYs) and mortality rates². Unfortunately, current therapies primarily manage PD symptoms, lacking the ability to slow or halt disease progression.

Parkinson's disease is characterized by both motor and non-motor features³. Motor symptoms like tremors, rigidity, bradykinesia (slowness of movement), and postural instability significantly impact patients' physical abilities. Additionally, PD can affect mental health by causing depression, anxiety, and cognitive impairment. These factors collectively contribute to a decline in quality of life, often leading to financial burdens associated with long-term care⁴.

How to cite: Irsal RAP, Gholam GM, Firdaus DA, Liwanda N, Chairunisa F. Molecular Docking and Dynamics of *Xylocarpus granatum* as A Potential Parkinson's Drug Targeting Multiple Enzymes. *Borneo J Pharm.* 2024;7(2):161-71. doi:10.33084/bjop.v7i2.6810

The cardinal motor features of PD arise from the degeneration of dopaminergic neurons in the substantia nigra, a critical brain region responsible for dopamine production. Dopamine is a vital neurotransmitter responsible for movement control. Three key enzymes – catechol-O-methyltransferase (COMT), monoamine oxidase-B (MAO-B), and adenosine A2A receptor (A2AR) – all play a role in regulating dopamine levels. COMT breaks down dopamine, MAO-B contributes to its degradation, and A2AR modulates dopamine release⁵⁻⁷.

The limitations of conventional therapies have spurred research into novel therapeutic approaches. Natural products, particularly those derived from plants, are a promising avenue for the development of new anti-Parkinson's agents. *Xylocarpus granatum* is a plant species that has attracted significant research interest due to its potential neuroprotective properties⁸. This activity may offer protection against the neuronal damage and degeneration characteristic of PD. Additionally, studies suggest that *X. granatum* possesses antidepressant-like effects in mice, potentially aiding in managing this common non-motor symptom in PD patients⁹. The reported pharmacological activities of *X. granatum* warrant further investigation into its potential as an anti-Parkinson's agent.

This study aims to elucidate the mechanism of action of an ethanol extract derived from *X. granatum* using computational approaches. We employ molecular docking and molecular dynamics simulations to investigate the interaction between this extract and three key enzymes implicated in PD pathogenesis: A2AR, COMT, and MAO-B. Molecular docking analysis provides insights into the binding interactions between the extract and these enzymes¹⁰. Subsequently, molecular dynamics simulations allow us to monitor the dynamic behavior and structural changes of the molecular complexes formed during these interactions¹¹.

MATERIALS AND METHODS

Materials

Three-dimensional structures of the target receptors, COMT, A2AR, and MAO-B enzymes, were retrieved from the RCSB Protein Data Bank (<https://www.rcsb.org/>) using the following PDB codes: 3BWM, 3PWH, and 2V61, respectively. 3D structures of the test compounds and natural ligands (used as controls) were obtained from PubChem (<https://pubchem.ncbi.nlm.nih.gov/>). Docking simulations were performed using YASARA Structure version 19.9.17 and BIOVIA Discovery Studio 2017 R2 Client 17.2. The computational hardware employed for these simulations consisted of an AMD Ryzen 5 3600 processor with 12 cores running at 3.6 GHz and 32 GB of RAM, operating under a Windows 11 Pro 64-bit operating system.

Methods

Preparation of receptors and ligands

Three-dimensional structures of all receptors were obtained from RCSB PDB in .pdb format. Water molecules and any nonessential residues were removed to prepare the protein structure for docking simulations. Hydrogen atoms were then added, and bond orders and hydrogenation states were adjusted using YASARA Structure to reflect a physiological pH of 7.4. This step ensures a more accurate representation of the *in vivo* environment where protein-ligand interactions occur. Thirty test compounds identified by Heryanto *et al.*¹² using GC/MS analysis were selected for docking simulations. The 3D structures of both the test compounds and a reference ligand (cite source of reference ligand) were retrieved from PubChem¹³. All ligand structures were prepared using YASARA Structure and underwent energy minimization to optimize atomic positions and obtain the lowest possible free energy state.

Molecular docking

Docking simulations were performed using the pre-configured script "dock_runscreening.mcr" within YASARA Structure. This script was executed 100 times to generate a statistically robust dataset of ligand-receptor interactions. The docking results were captured in .txt format for further analysis¹⁴. The docked ligand-receptor complexes were then analyzed using Discovery Studio to visualize and quantify the intermolecular interactions. This analysis focused on identifying and characterizing key interactions such as hydrogen bonds and hydrophobic interactions, which contribute to the binding

affinity between the ligand and receptor molecule. The visualization software allowed for the generation of two-dimensional interaction maps to depict these interactions in detail¹⁵.

Density functional theory analysis

Density functional theory (DFT) calculations were performed using Gaussian 09W software to optimize the geometries of the selected molecular structures. Geometry optimization employed the B3LYP functional and the 3-21G* basis set. Subsequently, the highest occupied molecular orbital (HOMO) and lowest unoccupied molecular orbital (LUMO) energies were calculated at the DFT level. These energy values served as the foundation for computing global chemical reactivity descriptors, including hardness (η), chemical potential (μ), softness (S), electronegativity (χ), and electrophilicity index (ω). All calculations adhered to the methodology established by Tamaciu *et al.*¹⁶. Equations 1 and 2 were utilized to calculate the electron affinity (A) and ionization potential (I), respectively. The chemical potential (μ), electronegativity (χ), hardness (η), softness (S), and electrophilicity index (ω) were computed using Equations 3 to 7, respectively.

$$I = -E_{HOMO} \quad [1]$$

$$A = -E_{LUMO} \quad [2]$$

$$\mu = -\frac{(I+A)}{2} \quad [3]$$

$$\chi = \frac{(I+A)}{2} \quad [4]$$

$$\eta = \frac{(I-A)}{2} \quad [5]$$

$$S = \frac{1}{2\mu} \quad [6]$$

$$\omega = \frac{\mu^2}{2\mu} \quad [7]$$

Molecular dynamics simulation

The docked protein-ligand complex PDB file was loaded into YASARA Structure. The molecular dynamics (MD) simulation was performed using the "md_run.mcr" macro within YASARA Structure, with modifications to extend the simulation duration to 50 ns. The simulated system was maintained at physiological conditions: 300 K temperature, pH 7.4, and 0.9% NaCl. Following completion of the initial MD simulation, the simulation was continued using the protein-ligand complex obtained at the end of the first run. The YASARA Structure "md_analyze.mcr" macro was employed with default settings to analyze the MD simulation trajectories. This analysis yielded RMSD, radius of gyration (Rg), and root mean square fluctuation (RMSF) values for the protein and ligand^{17,18}.

Data analysis

Ligand binding energy analysis during the MD simulation was performed using the built-in "md_analyzebindenergy.mcr" macro within YASARA Structure, which employs the Molecular Mechanics Poisson-Boltzmann Surface Area (MM-PBSA) calculation method¹⁷. Quantitative analysis of the simulation results and data visualization were conducted using Microsoft Excel. Binding energy calculations were based on the previously reported Equation 8 by Odhar *et al.*¹⁹.

$$\text{Binding Energy} = E_{\text{potRecept}} + E_{\text{solvRecept}} + E_{\text{potLigand}} + E_{\text{solvLigand}} - E_{\text{potComplex}} - E_{\text{solvComplex}} \quad [8]$$

RESULTS AND DISCUSSION

Virtual screening identified 30 potential inhibitors of three PD-linked enzymes from *X. granatum* ethanol extract. As expected, all control drugs displayed more favorable (more negative) Gibbs free energy (ΔG) values compared to the identified *X. granatum* compounds (Figure 1). However, three *X. granatum* compounds exhibited ΔG values approaching those of the controls, warranting further investigation through *in silico* approaches like DFT and MD simulations. The ΔG reflects the binding affinity between a ligand and its target enzyme. A more negative ΔG value signifies stronger binding and potentially greater inhibitory activity^{13,17}. While none of the identified *X. granatum* compounds surpassed the control

drugs in ΔG values, the three compounds identified for each enzyme show promise as potential alternative treatments. This highlights the importance of further exploration and development to exploit their therapeutic potential. Although not surpassing the controls, these *X. granatum* compounds with ΔG values approaching those of controls represent a promising starting point for discovering novel PD therapeutics.

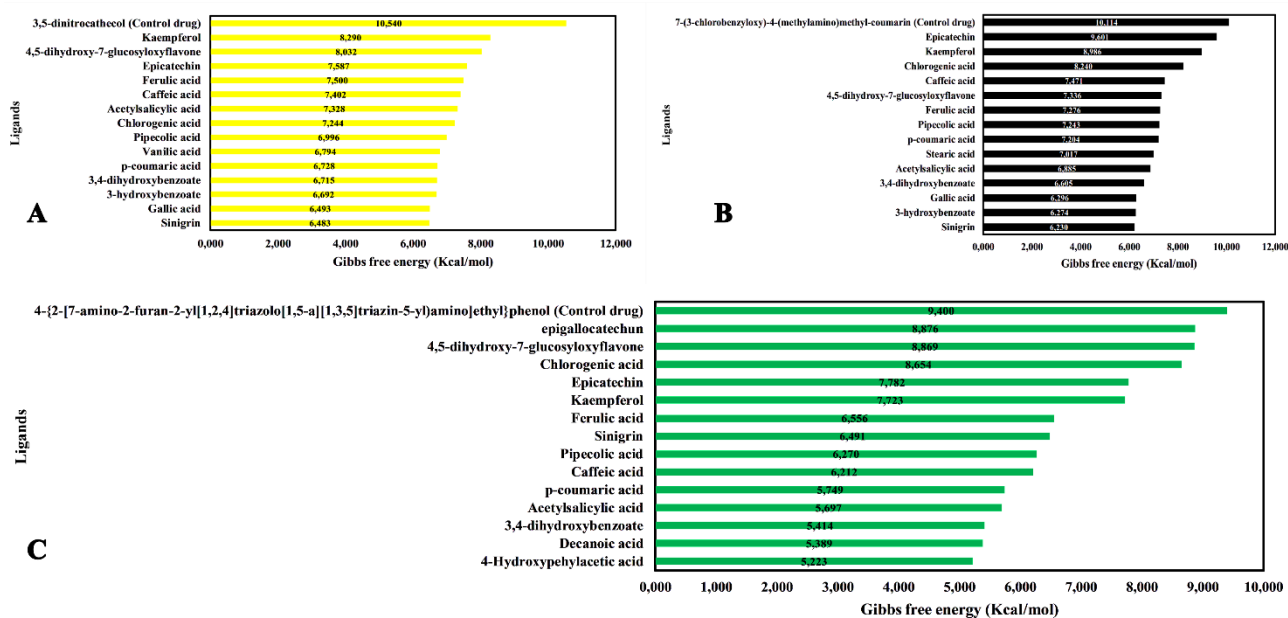


Figure 1. Changes in stability of PD enzymes in 50 ns. (a) MM-PBSA, (b) Rg, and (c) RMSD.

Docking simulations were performed to investigate the binding interactions between the top three identified compounds (epigallocatechin, kaempferol, and epicatechin) and three target enzymes: COMT, A2AR, and MAO-B (Figure 2). Each enzyme possesses distinct active site residues: COMT (ASP141, HIS142, TRP143, LYS144), A2AR (ALA63, GLU169, ASN253, ALA277, HIS278), and MAO-B (TYR60, PRO102, LEU164, PHE168, LEU171, CYS172, ILE198, ILE199, GLN206, TYR326, PHE343). Epigallocatechin interacted with the active site of A2AR (GLU169, ASN253, HIS278) via a hydrogen bond with ASN253 and van der Waals interactions elsewhere. The control drug for A2AR bound to four residues (ALA63, GLU169, ASN253, HIS278) but lacked a hydrogen bond with ASN253, relying solely on van der Waals interactions, which may be less favorable for binding affinity.

Kaempferol formed hydrophobic interactions with two COMT active site residues (HIS142 and TRP143). The control drug for COMT interacted with all COMT active sites, exhibiting various interactions (salt bridge, hydrogen bond, hydrophobic, and van der Waals). However, the interaction with ASP141 might be unfavorable. Epicatechin bound to seven COMT active sites (TYR60, LEU171, CYS172, ILE198, ILE199, TYR326, and PHE343), forming a combination of three hydrogen bonds, two hydrophobic interactions, and two van der Waals interactions. The control drug for COMT interacted with all active sites, exhibiting one hydrogen bond, one pi-sulfur bond, one attractive charge interaction, five hydrophobic interactions, and van der Waals interactions with the remaining residues.

In this study, hydrogen bonds (conventional and carbon-hydrogen) and hydrophobic interactions were observed, contributing to the overall binding strength of the ligand-enzyme complexes. Generally, a higher number of hydrogen bonds and hydrophobic interactions correlate with increased binding energy²⁰. However, our findings also revealed the presence of an unfavorable negative-negative interaction between the control drug for A2AR (4-{2-[7-amino-2-furan-2-yl][1,2,4]triazolo[1,5-a][1,3,5]triazin-5-yl]amino}ethyl]phenol) and epigallocatechin, potentially affecting drug activity due to repulsive forces between atoms²¹. Overall, the three test ligands derived from *X. granatum* displayed distinct binding characteristics, warranting further investigation using molecular dynamics simulations to assess the stability of these complexes.

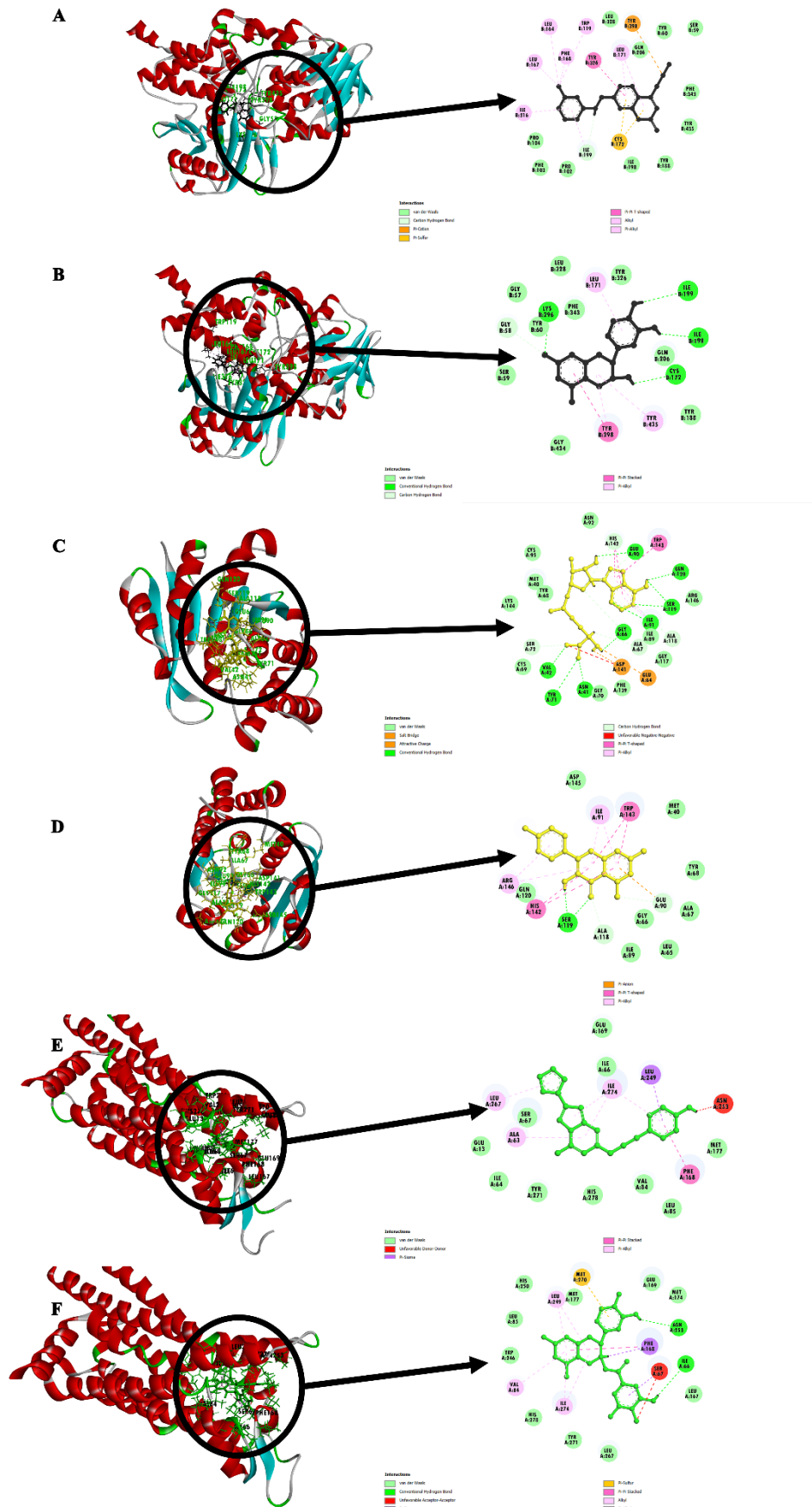


Figure 2. Docked ligand-receptor complexes of (A) 7-(3-chlorobenzoyloxy)-4-(methylamino)methyl-coumarin-MAOB, (B) epicatechin-MAOB, (C) 3,5-dinitrocatechol-COMT, (D) kaempferol-COMT, (E) 4-[2-[7-amino-2-furan-2-yl][1,2,4]triazolo[1,5-a][1,3,5]triazin-5-yl]amino]ethylphenol-A2AR, (F) epigallocatechin-A2AR.

Density functional theory calculations were performed to investigate the electronic properties of the three identified compounds (kaempferol, epicatechin, and epigallocatechin) (Figure 3). The HOMO-LUMO energy gap, an indicator of molecular softness, was calculated. Kaempferol exhibited the most negative energy gap (-0.27408 eV), followed by epicatechin (-0.20037 eV) and epigallocatechin (-0.20673 eV). A lower energy gap corresponds to a softer molecule. The complete summary of DFT calculations is presented in Table I. Notably, all three ligands displayed a favorable characteristic: low hardness combined with high softness, suggesting their potential as promising phytochemicals.

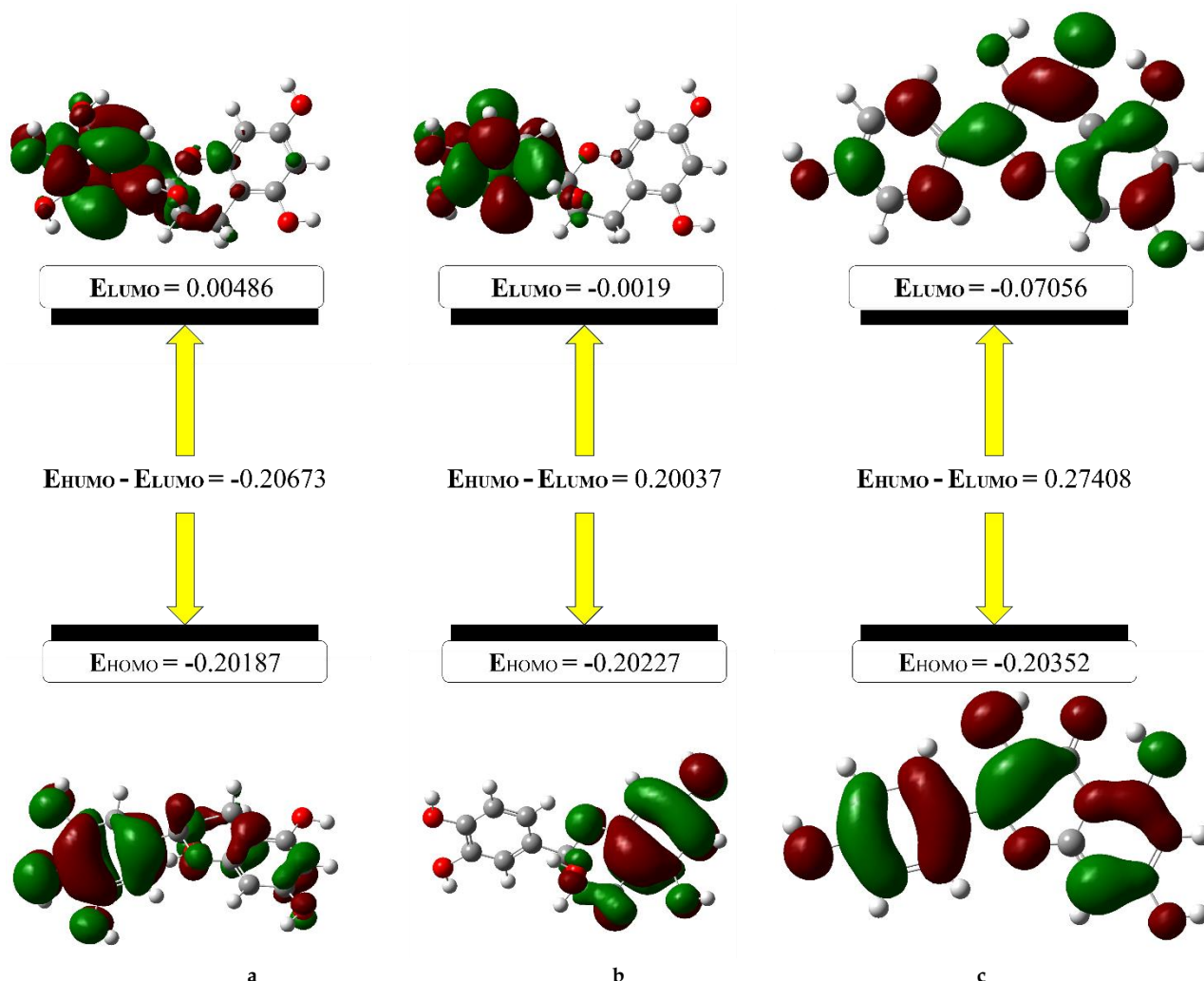


Figure 3. Visualization of HOMO, LUMO, and energy gap of selected compounds which were further analyzed with DFT. (a) epigallocatechin, (b) epicatechin, and (c) kaempferol.

Table I. Calculation analysis of DFT studies on selected compounds.

Compounds	EHOMO (eV)	ELUMO (eV)	Energy gap (eV)	Ionization potential (eV)	Affinity (eV)	Chemical potential (eV)	Electronegativity (eV)	Hardness (eV)	Softness (eV)	Electrophilicity index (eV)
Epicatechin	-0.20227	-0.0019	-0.20037	0.20227	0.0019	-0.102085	0.102085	0.100185	4.99077	0.05326
Kaempferol	-0.20352	-0.07056	-0.27408	0.20352	0.07056	-0.13704	0.13704	0.06648	7.52106	0.14124
Epigallocatechin	-0.20187	0.00486	-0.20673	0.20187	-0.00486	-0.098505	0.098505	0.103365	4.82393	0.04694

Frontier molecular orbitals (HOMO and LUMO) were investigated to gain insights into the optical, electrical properties, and potential interactions of the studied compounds (kaempferol, epicatechin, and others). Additionally, the HOMO-LUMO ΔG , η , μ , S , χ , and ω were calculated to further explore their electronic properties and chemical reactivity. The ΔG reflects compound stability, with a larger gap indicating greater stability. Based on the calculated ΔG values, kaempferol was predicted to be the most stable compound. The μ reflects the tendency of a molecule to lose or gain electrons. Both η and S are interrelated and describe the ease of electron donation or acceptance, respectively, influencing reactivity. Ionization

potential and electron affinity are crucial parameters for calculating χ and absolute η . Finally, ω indicates the electron-accepting tendency of a molecule. Collectively, these frontier molecular orbital parameters provide valuable insights into various aspects of the studied compounds, aiding in the identification of potential drug candidates or enzyme inhibitors^{16,22-24}.

Ligand binding to a receptor can induce subtle but significant changes in the receptor's structure. In this study, we investigated these alterations by analyzing RMSF of the active-site residues in the complexes formed between kaempferol, epicatechin, and their native ligands with COMT, A2AR, and MAO-B enzymes over a 50 ns molecular dynamics simulation. The RMSF serves as a measure of protein structural flexibility, with higher values indicating greater mobility. The RMSF values for the active-site residues (**Table II**) are particularly noteworthy. Notably, the complexes formed by kaempferol, epicatechin, and their native ligands with COMT and MAO-B enzymes exhibit minimal RMSF values, suggesting robust stability within the protein-ligand interactions. As reported by Dash *et al.*²⁵, RMSF calculations capture the dynamic behavior of protein backbones, with elevated values indicating increased flexibility. Furthermore, Biswas *et al.*²⁶ proposed that ligand-protein complexes with RMSF values below 1.4 Å for each residue suggest a stable interaction. Gratifyingly, all our tested ligand complexes satisfy this criterion, indicating favorable protein-ligand binding.

Table II. RMSF of PD-linked enzymes active sites.

A2AR			COMT			MAO-B		
Residues	Epigallocatechin	4-[2-[(7-amino-2-furan-2-yl)[1,2,4]triazolo[1,5-a][1,3,5]triazin-5-yl)amino]ethyl]phenol	Residues	Kaempferol	3,5-dinitrocathecol	Residues	3,5-dinitrocathecol	7-(3-chlorobenzyloxy)-4-(methylamino)methylcoumarin
ALA163	1.803	1.060	ASP141	0.604	0.599	TYR60	0.601	0.655
GLU169	1.573	1.301	HIS142	0.525	0.643	PRO102	0.823	0.859
ASN253	1.64	1.459	TRP143	0.920	1.035	LEU164	0.965	1.056
ALA277	1.078	0.903	LYS144	0.832	0.891	PHE168	0.646	0.605
HIS278	1.977	1.389	-	-	-	LEU171	0.712	0.648
-	-	-	-	-	-	CYS172	1.332	1.644
-	-	-	-	-	-	ILE198	1.025	1.234
-	-	-	-	-	-	ILE199	0.459	0.524
-	-	-	-	-	-	GLN206	0.563	0.467
-	-	-	-	-	-	TYR326	0.532	0.674
-	-	-	-	-	-	PHE343	0.448	0.454

Molecular dynamics simulations revealed ligand-induced alterations in protein backbone flexibility. The RMSF values indicated minimal fluctuations in the active site residues of complexes with kaempferol, epicatechin, and native ligands, suggesting stable protein-ligand interactions (**Figure 4A**). This aligns with the proposed stability criteria²⁶ and findings by Dash *et al.*²⁵. These minimal RMSF values suggest favorable interactions between the studied compounds and their target enzymes, COMT and MAO-B, potentially influencing their effectiveness as inhibitors or modulators.

Free energy calculations from MM-PBSA simulations provided insights into ligand binding affinities (**Figure 4A**). Positive ΔG values suggest favorable binding, consistent with YASARA's methodology²⁷. Notably, kaempferol displayed a higher ΔG than the natural ligand for COMT, indicating a potentially stronger interaction. This finding highlights kaempferol's promise for further investigation in drug development. Overall, the positive ΔG values suggest that the studied compounds form stable complexes with their respective enzymes, supporting their potential as therapeutic candidates.

The Rg values provided insights into protein complex structures (**Figure 4B**). Control drug-MAO-B exhibited a higher Rg value, indicating a looser protein structure compared to other complexes. This aligns with Dash *et al.*²⁵ and suggests increased flexibility. The Rg serves as a measure of protein compactness, offering a valuable indicator for biological contexts. In this study, Rg facilitated a comparative analysis of protein structures relative to their hydrodynamic radius. As highlighted by Justino *et al.*²⁸, Rg measurements contribute to our understanding of protein-environment interactions.

Stability of ligand binding modes is crucial for reliable MD simulations. The RMSD of the protein backbone in the final 5 ns of the simulation was used to assess stability (defined as RMSD < 2 Å) based on criteria from Chairunisa *et al.*¹⁸ (**Figure 4C**). All complexes, except two binding A2AR, exhibited stability with consistently low RMSD values throughout the 50 ns simulation. This collectively suggests structural stabilization of the ligand-protein complex, supported by the lower RMSD values observed in ligand-docked proteins compared to their unbound counterparts²⁹. The observed stability underscores the robustness of the MD simulations and the validity of the ligand binding modes.

This study employed a computational approach to investigate the interactions between the ethanol extract of *X. granatum* and potential anti-Parkinson's targets. The findings provide insights into ligand-induced protein flexibility changes, binding affinities, and structural stability. Notably, kaempferol displayed promising potential as a COMT inhibitor. We believe this work contributes valuable information for the development of more effective PD treatments.

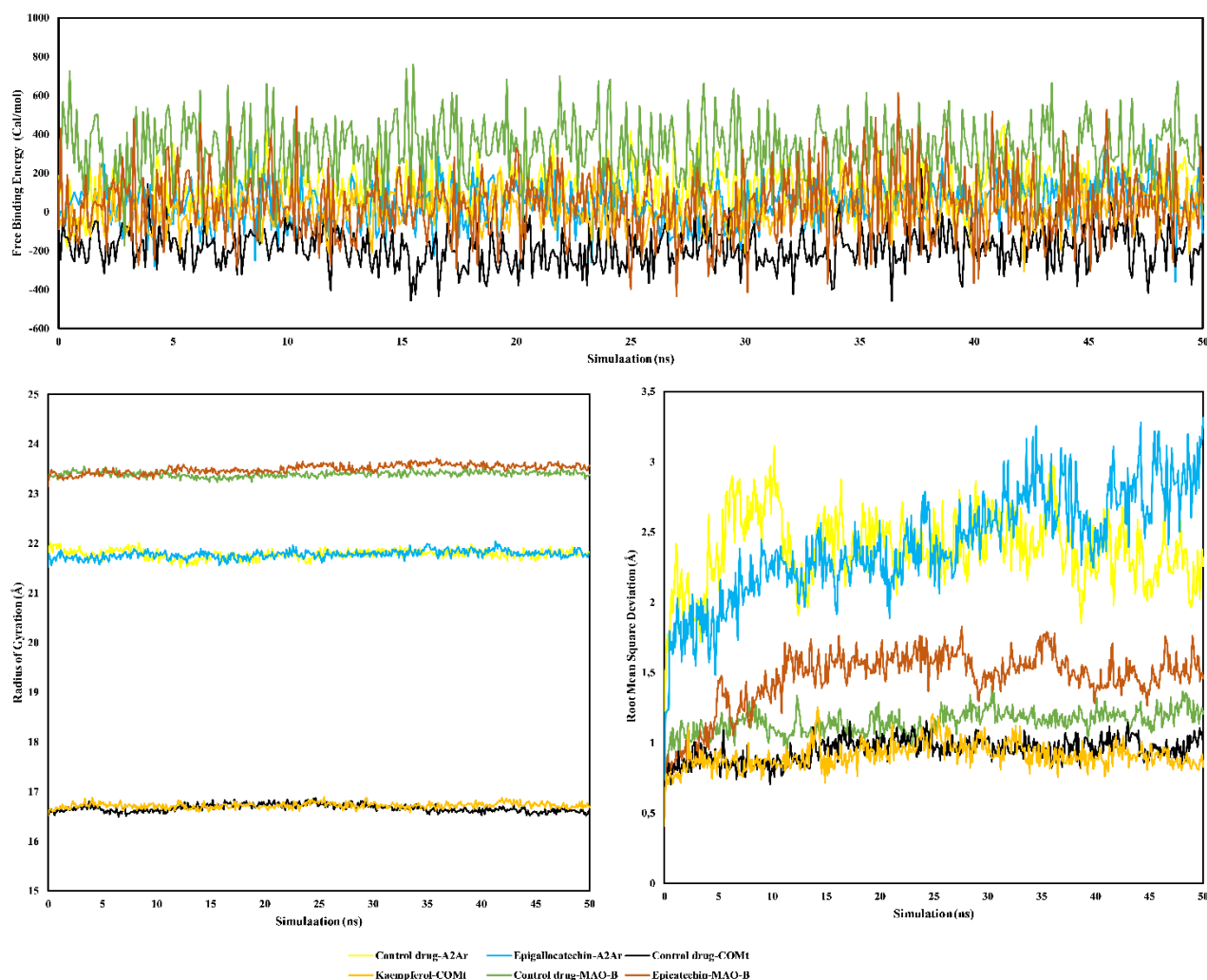


Figure 4. Changes in stability of PD enzymes in 50 ns. (a) MM-PBSA, (b) Rg, and (c) RMSD.

CONCLUSION

In silico docking simulations identified several *X. granatum* compounds with promising binding affinities to A2AR, COMT, and MAO-B, key enzymes implicated in PD. Notably, five compounds exhibited high binding energies to each target protein: A2AR (epigallocatechin, 4,5-dihydroxy-7-glucoloxylflavonone, chlorogenic acid, epicatechin, and kaempferol), COMT (kaempferol, 4,5-dihydroxy-7-glucoloxylflavonone, epigallocatechin, epicatechin, and ferulic acid), and MAO-B (epicatechin, kaempferol, chlorogenic acid, caffeic acid, and stearic acid). Analysis of the MAO-B-ligand complex revealed a more flexible protein conformation, potentially enhancing ligand binding. Overall stability of the ligand-protein interactions was confirmed by RMSD analysis, except for the A2AR complex, which may warrant further investigation. These findings suggest that *X. granatum* may possess structural stabilization effects on key PD-related proteins, highlighting its potential as a therapeutic candidate. Future studies exploring *in vitro* and *in vivo* models are warranted to validate these *in silico* observations and elucidate the precise mechanisms of action. This research offers valuable insights that could pave the way for the development of novel and more effective therapies for PD.

ACKNOWLEDGMENT

This research received no external funding.

AUTHORS' CONTRIBUTION

Conceptualization: Riyan Alifbi Putera Irsal, Gusnia Meilin Gholam

Data curation: Riyan Alifbi Putera Irsal, Gusnia Meilin Gholam, Dzikri Anfasa Firdaus, Novian Liwanda, Fernanda Chairunisa

Formal analysis: Riyan Alifbi Putera Irsal, Gusnia Meilin Gholam, Dzikri Anfasa Firdaus, Novian Liwanda, Fernanda Chairunisa

Funding acquisition: -

Investigation: Riyan Alifbi Putera Irsal, Gusnia Meilin Gholam

Methodology: Riyan Alifbi Putera Irsal, Gusnia Meilin Gholam

Project administration: Riyan Alifbi Putera Irsal, Gusnia Meilin Gholam

Resources: Riyan Alifbi Putera Irsal, Gusnia Meilin Gholam, Fernanda Chairunisa

Software: Riyan Alifbi Putera Irsal, Gusnia Meilin Gholam

Supervision: Riyan Alifbi Putera Irsal, Gusnia Meilin Gholam, Dzikri Anfasa Firdaus, Novian Liwanda, Fernanda Chairunisa

Validation: Riyan Alifbi Putera Irsal, Gusnia Meilin Gholam, Fernanda Chairunisa

Visualization: Riyan Alifbi Putera Irsal, Gusnia Meilin Gholam

Writing - original draft: Riyan Alifbi Putera Irsal, Gusnia Meilin Gholam

Writing - review & editing: Riyan Alifbi Putera Irsal, Gusnia Meilin Gholam, Dzikri Anfasa Firdaus, Novian Liwanda, Fernanda Chairunisa

DATA AVAILABILITY

All of the data is contained within this manuscript.

CONFLICT OF INTEREST

The authors declare no conflicts of interest.

REFERENCES

1. Ou Z, Oan J, Tang S, Duan D, Yu D, Nong H, et al. Global Trends in the Incidence, Prevalence, and Years Lived with Disability of Parkinson's Disease in 204 Countries/Territories From 1990 to 2019. *Front Public Health*. 2021;9:776847. DOI: [10.3389/fpubh.2021.776847](https://doi.org/10.3389/fpubh.2021.776847); PMCID: [PMC8688697](https://pubmed.ncbi.nlm.nih.gov/34950630/); PMID: [34950630](https://pubmed.ncbi.nlm.nih.gov/34950630/)
2. Kouli A, Torsney KM, Kuan WL. Parkinson's Disease: Etiology, Neuropathology, and Pathogenesis. In: Stoker TB, Greenland JC, editors. *Parkinson's Disease: Pathogenesis and Clinical Aspects*. Brisbane (AU): Codon Publications; 2018. DOI: [10.15586/codonpublications.parkinsonsdisease.2018.ch1](https://doi.org/10.15586/codonpublications.parkinsonsdisease.2018.ch1)
3. DeMaagd G, Philip A. Parkinson's Disease and Its Management: Part 1: Disease Entity, Risk Factors, Pathophysiology, Clinical Presentation, and Diagnosis. *P T*. 2015;40(8):504-32. PMCID: [PMC4517533](https://pubmed.ncbi.nlm.nih.gov/26236139/); PMID: [26236139](https://pubmed.ncbi.nlm.nih.gov/26236139/)

4. Magrinelli F, Picelli A, Tocco P, Federico A, Roncari L, Smania N, et al. Pathophysiology of Motor Dysfunction in Parkinson's Disease as the Rationale for Drug Treatment and Rehabilitation. *Parkinsons Dis.* 2016;2016:9832839. DOI: [10.1155/2016/9832839](https://doi.org/10.1155/2016/9832839); PMCID: [PMC4913065](https://pubmed.ncbi.nlm.nih.gov/PMC4913065/); PMID: [27366343](https://pubmed.ncbi.nlm.nih.gov/27366343/)
5. Jankovic J, Tan EK. Parkinson's disease: etiopathogenesis and treatment. *J Neurol Neurosurg Psychiatry.* 2020;91(8):795-808. DOI: [10.1136/jnnp-2019-322338](https://doi.org/10.1136/jnnp-2019-322338); PMID: [32576618](https://pubmed.ncbi.nlm.nih.gov/32576618/)
6. Regensburger M, Ip CW, Kohl Z, Schrader C, Urban PP, Kassubek J, et al. Clinical benefit of MAO-B and COMT inhibition in Parkinson's disease: practical considerations. *J Neural Transm.* 2023;130(6):847-61. DOI: [10.1007/s00702-023-02623-8](https://doi.org/10.1007/s00702-023-02623-8); PMCID: [PMC10199833](https://pubmed.ncbi.nlm.nih.gov/PMC10199833/); PMID: [36964457](https://pubmed.ncbi.nlm.nih.gov/36964457/)
7. Boulaamane Y, Ibrahim MAA, Britel MR, Maurady A. In silico studies of natural product-like caffeine derivatives as potential MAO-B inhibitors/AA 2A R antagonists for the treatment of Parkinson's disease. *J Integr Bioinform.* 2022;19(4):20210027. DOI: [10.1515/jib-2021-0027](https://doi.org/10.1515/jib-2021-0027); PMCID: [PMC9800045](https://pubmed.ncbi.nlm.nih.gov/PMC9800045/); PMID: [36112816](https://pubmed.ncbi.nlm.nih.gov/36112816/)
8. Dey D, Quispe C, Hossain R, Jain D, Ahmed Khan R, Janmeda P, et al. Ethnomedicinal Use, Phytochemistry, and Pharmacology of *Xylocarpus granatum* J. Koenig, Emran T Bin, editor. *Evid Based Complement Altern Med.* 2021;2021:8922196. DOI: [10.1155/2021/8922196](https://doi.org/10.1155/2021/8922196); PMCID: [PMC8423563](https://pubmed.ncbi.nlm.nih.gov/PMC8423563/); PMID: [34504541](https://pubmed.ncbi.nlm.nih.gov/34504541/)
9. Yin X, Li X, Hao Y, Zhao Y, Zhou J, Shi H. Xylocarpin H, a Limonoid of *Xylocarpus granatum*, Produces Antidepressant-Like Activities in Mice. *J Behav Brain Sci.* 2015;5(11):524-32. DOI: [10.4236/jbbs.2015.511050](https://doi.org/10.4236/jbbs.2015.511050)
10. Agu PC, Afiukwa CA, Orji OU, Ezeh EM, Ofoke IH, Ogbu CO, et al. Molecular docking as a tool for the discovery of molecular targets of nutraceuticals in diseases management. *Sci Rep.* 2023;13(1):13398. DOI: [10.1038/s41598-023-40160-2](https://doi.org/10.1038/s41598-023-40160-2); PMCID: [PMC10435576](https://pubmed.ncbi.nlm.nih.gov/PMC10435576/); PMID: [37592012](https://pubmed.ncbi.nlm.nih.gov/37592012/)
11. Hollingsworth SA, Dror RO. Molecular Dynamics Simulation for All. *Neuron.* 2018;99(6):1129-43. DOI: [10.1016/j.neuron.2018.08.011](https://doi.org/10.1016/j.neuron.2018.08.011); PMCID: [PMC6209097](https://pubmed.ncbi.nlm.nih.gov/PMC6209097/); PMID: [30236283](https://pubmed.ncbi.nlm.nih.gov/30236283/)
12. Heryanto R, Putra CA, Khalil M, Rafi M, Putri SP, Karomah AH, et al. Antioxidant Activity and Metabolite Profiling of *Xylocarpus granatum* Extracts Using Gas Chromatography-Mass Spectrometry. *Metabolites.* 2023;13(2):156. DOI: [10.3390/metabo13020156](https://doi.org/10.3390/metabo13020156); PMCID: [PMC9958973](https://pubmed.ncbi.nlm.nih.gov/PMC9958973/); PMID: [36837775](https://pubmed.ncbi.nlm.nih.gov/36837775/)
13. Irsal RAP, Seno DSH, Safithri M, Kurniasih R. Penapisan Virtual Senyawa Aktif Sirih Merah (*Piper Crocatum*) sebagai Inhibitor Angiotensin Converting Enzyme. *J Farmamedika Pharmamedika J.* 2022;7(2):104-13. DOI: [10.47219/ath.v7i2.157](https://doi.org/10.47219/ath.v7i2.157)
14. Durai P, Shin H, Achek A, Kwon H, Govindaraj RG, Panneerselvam S, et al. Toll-like receptor 2 antagonists identified through virtual screening and experimental validation. *FEBS J.* 2017;284(14):2264-83. DOI: [10.1111/febs.14124](https://doi.org/10.1111/febs.14124); PMID: [28570013](https://pubmed.ncbi.nlm.nih.gov/28570013/)
15. Gholam GM, Darmawan NI, Siregar JE, Artika IM. Selected Polyphenols from Date (*Phoenix dactylifera*) as Anti-Virulence of *Candida albicans* Through Multiple Enzyme Targets. *Biointerface Res Appl Chem.* 2022;13(4):386. DOI: [10.33263/BRIAC134.386](https://doi.org/10.33263/BRIAC134.386)
16. Talmaciu MM, Bodoki E, Oprean R. Global chemical reactivity parameters for several chiral beta-blockers from the Density Functional Theory viewpoint. *Clujul Med.* 2016;89(4):513-8. DOI: [10.15386/cjmed-610](https://doi.org/10.15386/cjmed-610); PMCID: [PMC5111492](https://pubmed.ncbi.nlm.nih.gov/PMC5111492/); PMID: [27857521](https://pubmed.ncbi.nlm.nih.gov/27857521/)
17. Land H, Humble MS. YASARA: A Tool to Obtain Structural Guidance in Biocatalytic Investigations. In: Bornscheuer UT, Höhne M, editors. *Protein Engineering. Methods in Molecular Biology.* New York (US): Humana Press; 2018. p. 43-67. DOI: [10.1007/978-1-4939-7366-8_4](https://doi.org/10.1007/978-1-4939-7366-8_4)
18. Chairunisa F, Safithri M, Andrianto D, Kurniasih R, Irsal RAP. Molecular Docking of Red Betel Leaf Bioactive Compounds (*Piper crocatum*) as Lipoyxygenase Inhibitor. *Indones J Pharm Sci Technol.* 2023;10(2):90-103. DOI: [10.24198/ijpst.v10i2.38934](https://doi.org/10.24198/ijpst.v10i2.38934)

19. Odhar HA, Hashim AF, Humad SS. Molecular docking analysis and dynamics simulation of salbutamol with the monoamine oxidase B (MAO-B) enzyme. *Bioinformation*. 2022;18(3):304-9. DOI: [10.6026/97320630018304](https://doi.org/10.6026/97320630018304); PMCID: [PMC9722423](https://pubmed.ncbi.nlm.nih.gov/36518132/); PMID: [36518132](https://pubmed.ncbi.nlm.nih.gov/36518132/)
20. Ferenczy GG, Kellermayer M. Contribution of hydrophobic interactions to protein mechanical stability. *Comput Struct Biotechnol J*. 2022;20:1946-56. DOI: [10.1016/j.csbj.2022.04.025](https://doi.org/10.1016/j.csbj.2022.04.025); PMCID: [PMC9062142](https://pubmed.ncbi.nlm.nih.gov/35521554/); PMID: [35521554](https://pubmed.ncbi.nlm.nih.gov/35521554/)
21. Dhorajiwala TM, Halder ST, Samant L. Computer-Aided Docking Studies of Phytochemicals from Plants *Salix Subserata* and *Onion* as Inhibitors of Glycoprotein G of Rabies Virus. *Biomed Biotechnol Res J*. 2019;3(4):269-76. DOI: [10.4103/bbrj.bbrj_124_19](https://doi.org/10.4103/bbrj.bbrj_124_19)
22. Roohi H, Mohtamadifar N. The role of the donor group and electron-accepting substitutions inserted in π -linkers in tuning the optoelectronic properties of D- π -A dye-sensitized solar cells: a DFT/TDDFT study. *RSC Adv*. 2022;12(18):11557-73. DOI: [10.1039/d2ra00906d](https://doi.org/10.1039/d2ra00906d); PMCID: [PMC9006569](https://pubmed.ncbi.nlm.nih.gov/35425060/); PMID: [35425060](https://pubmed.ncbi.nlm.nih.gov/35425060/)
23. Chattaraj PK, Duley S. Electron Affinity, Electronegativity, and Electrophilicity of Atoms and Ions†. *J Chem Eng Data*. 2010;55(5):1882-6. DOI: [10.1021/je900892p](https://doi.org/10.1021/je900892p)
24. Zhan CG, Nichols JA, Dixon DA. Ionization Potential, Electron Affinity, Electronegativity, Hardness, and Electron Excitation Energy: Molecular Properties from Density Functional Theory Orbital Energies. *J Phys Chem A*. 2003;107(20):4184-95. DOI: [10.1021/jp0225774](https://doi.org/10.1021/jp0225774)
25. Dash R, Ali MC, Dash N, Azad MAK, Hosen SMZ, Hannan MA, et al. Structural and Dynamic Characterizations Highlight the Deleterious Role of SULT1A1 R213H Polymorphism in Substrate Binding. *Int J Mol Sci*. 2019;20(24):6256. DOI: [10.3390/ijms20246256](https://doi.org/10.3390/ijms20246256); PMCID: [PMC6969939](https://pubmed.ncbi.nlm.nih.gov/31835852/); PMID: [31835852](https://pubmed.ncbi.nlm.nih.gov/31835852/)
26. Biswas S, Mahmud S, Mita MA, Afrose S, Hasan MR, Shimu MSS, et al. Molecular Docking and Dynamics Studies to Explore Effective Inhibitory Peptides Against the Spike Receptor Binding Domain of SARS-CoV-2. *Front Mol Biosci*. 2022;8(10):1305-15. DOI: [10.3389/fmolb.2021.791642](https://doi.org/10.3389/fmolb.2021.791642); PMCID: [PMC8851422](https://pubmed.ncbi.nlm.nih.gov/35187069/); PMID: [35187069](https://pubmed.ncbi.nlm.nih.gov/35187069/)
27. Genheden S, Ryde U. The MM/PBSA and MM/GBSA methods to estimate ligand-binding affinities. *Expert Opin Drug Discov*. 2015;10(5):449-61. DOI: [10.1517/17460441.2015.1032936](https://doi.org/10.1517/17460441.2015.1032936); PMCID: [PMC4487606](https://pubmed.ncbi.nlm.nih.gov/25835573/); PMID: [25835573](https://pubmed.ncbi.nlm.nih.gov/25835573/)
28. Justino GC, Nascimento CP, Justino MC. Molecular dynamics simulations and analysis for bioinformatics undergraduate students. *Biochem Mol Biol Educ*. 2021;49(4):570-82. DOI: [10.1002/bmb.21512](https://doi.org/10.1002/bmb.21512); PMID: [33844418](https://pubmed.ncbi.nlm.nih.gov/33844418/)
29. Ng HW, Laughton CA, Doughty SW. Molecular dynamics simulations of the adenosine A2a receptor: structural stability, sampling, and convergence. *J Chem Inf Model*. 2013;53(5):1168-78. DOI: [10.1021/ci300610w](https://doi.org/10.1021/ci300610w); PMID: [23514445](https://pubmed.ncbi.nlm.nih.gov/23514445/)